Phenomenological description of deadlock formation in pedestrian bidirectional flow based on empirical observation

Claudio Feliciani [1] and Katsuhiro Nishinari [1,2]

[1] Research Center for Advanced Science and Technology, The University of Tokyo, 4-6-1 Komaba, Meguro-ku, Tokyo 153-8904, Japan

[2] Department of Aeronautics and Astronautics, Graduate School of Engineering, The University of Tokyo, 7-3-1 Hongo, Bunkyo-ku, Tokyo 113-8656, Japan

E-mail: feliciani@jamology.rcast.u-tokyo.ac.jp

18 August 2015

Abstract. This article presents an empirical investigation for the phenomenon of deadlock formation by analyzing a pedestrian bidirectional flow of a subway station in central Tokyo. Using video images obtained from cameras placed in the station during morning rush hour, the in- and outflow (making up the total flow) resulting in a test section considered were computed. With the use of additional information such as the train arrival time, test section density and its flow ratio, the formation of different complex crowd phenomena is analyzed. The information provided by the unsteady flow curves allowed a qualitative and quantitative distinction between free flow, congested flow and deadlock formation. This latter phenomenon could be easily identified based on the shape of the total outflow showing a double peak. Based on the information gained, a flow regime diagram using flow and counter-flow values to distinguish between different flow regimes in bidirectional flow has been derived. In this regard, flow ratio was confirmed being a relevant parameter to describe bidirectional flow, providing experimental evidence that total flow alone can be misleading. Qualitative and quantitative results obtained in the present study were finally compared with previous literature showing good agreement.

1. Introduction

With human population shifting from countryside areas to urban center, cities are getting bigger and their population density increasingly higher. Transportation network is therefore under constant pressure and crowds of people are becoming difficult to control. In addition, international events (Olympics, World's fair,...) easily gather a large number of people and managing the crowd in case of accidents or unexpected events can be a challenging task for the security personnel involved. In fact, a poor crowd management can lead to devastating consequences as several accidents in the past demonstrated [1, 2].

For the above reasons, the understanding of the dynamic of human crowd is an important step to develop methods which may help in predicting dangerous situations. However, the study of pedestrian crowd under critic conditions is limited by several factors. The first limiting factor lies in the fact that during experiments it is not possible to recreate dangerous scenarios because of safety and ethical concerns. As a second factor, given the organizational burdens related to gathering several hundreds of people, experiments are usually carried out for small groups of people at low densities. In addition, people aware of taking part to an experiment may behave in a different way compared to a real case. As a last point, the use of images from surveillance cameras is usually difficult due to privacy violation concerns.

As a consequence of the above points, research on high density crowd behavior is usually performed either using animals or numerical codes. Concerning animals, studies involving ants [3, 4], sheep [5] and mouses [6] were reported. Computer codes are usually divided into continuous models (fluid dynamic model [7] and social force model [8] being the most famous) and discrete models (cellular automata [9] and multi-agent systems [10] among the most commonly used).

In addition, research on granular matter helped in some extent to deepen the understanding of multibody dynamics, with pedestrian behavior research benefiting from some of its applications.

To validate theoretical and numerical results humans were actually used experimentally in several studies [11, 12, 13, 14], but mostly using supervised experiments and with a limited number of people. Studies based on real-life observations have also been published [15, 11, 16, 17], but only for relatively low density crowds.

Here, in contrast to the previous studies, we had the opportunity to study a large number of people in a natural context for densities higher than the ones reported in the past literature. In particular, in this research we report the deadlock ‡ formation in a pedestrian bidirectional flow by observing passengers exchanging train line in a congested subway station during morning rush hour.

2. Experiment description

2.1. Experimental setup

The Omote-sando subway station in central Tokyo was chosen for this observation. This particular station was chosen for multiple reasons. First, several passengers reported being stuck in a crowd while exchanging line in that station, thus suggesting the formation of a dense crowd (and possibly deadlocks). Second, the authors witnessed on several occasions the creation of deadlocks in a clearly defined space in the reported subway station, thus providing ideal conditions for the empirical observation of the phenomenon. Lastly, the compact size of the station and its limited number of entrances

‡ Some authors use the term deadlock to refer to a complete stop of the crowd. In this study we will talk about deadlock referring to the event in which several pedestrians have to stop or significantly slow down to avoid collisions with the counter flow.

and exits gives the opportunity to accurately count the passengers moving in each direction.

The selected station has a daily ridership of more than 150,000 people [18] making it among the 20 most crowded subway stations in Tokyo. As schematically indicated in Figure 1, 3 lines are running through it, namely the Hanzomon and Ginza lines (running parallel in the vertical direction on the diagram) and the Chiyoda line (running horizontally on the diagram). Each train platform is connected with the main floor (located between the 3 lines) by means of stairs and escalators as indicated in the schematic image. In the main floor a large concourse area connects all the three lines allowing passengers to leave/enter the station and exchange line/platform on the same common floor. When passengers exchange the train from the Chiyoda line and move to the left side of Figure 1 to ride either the Ginza or the Hanzomon line, a dense crowd is formed in the narrow region highlighted in red. Analogously, the same phenomenon happens in the opposite direction, i.e. when passengers move from the left to the right side of the concourse to ride a train on the Chiyoda line. From now on, to simplify the notation, we will refer to the left side of the concourse as concourse A and to the right side as concourse B. The narrow passage on which this study is based lies between both sides of the concourse (thus between A and B).

Cameras were located in each strategic location in order to count for the number of people leaving each platform, entering/exiting the station and passing through the narrow section. Cameras numbered from 1 to 4 were placed to count the number of people leaving/entering each platform on concourse A, cameras 7 and 8 to count the people moving in/out concourse B (from/to the corresponding platform) and camera 5, 6 and 9 were placed at the entrance/exit of the station to count the people leaving/entering it. Finally cameras 10 and 11 were used to directly observe the formation of a dense crowd in the narrow section.

In the morning of December 18th, 2014 (Thursday) the movement of the passengers inside the station was recorded using the 11 cameras from slightly earlier than 7 AM during a roughly 2 hours period (until slightly later than 9 AM). Personnel of the train station supervised the operation to check that each camera was constantly pointing in the predetermined direction and to precisely adjust each camera's time to have a perfect synchronization between them.

In addition, detailed information containing the scheduled and effective arrival and departure time for each train on each platform was provided from the operator of the station (Tokyo Metro Co.,Ltd). This allowed us to compute the delay of each train and the arrival delay between trains on different platforms and in particular between both sides of the concourse.

Considering the low ceiling of the subway station (less than 3.0 m), each camera had to be set at low angle and, in some cases, they were looking frontally to the passengers. This fact, and the relative long distance from which people were observed, prevented the use of an automated video processing technique to count pedestrians. In addition, because of the time of the day considered, the vast majority of people were commuting

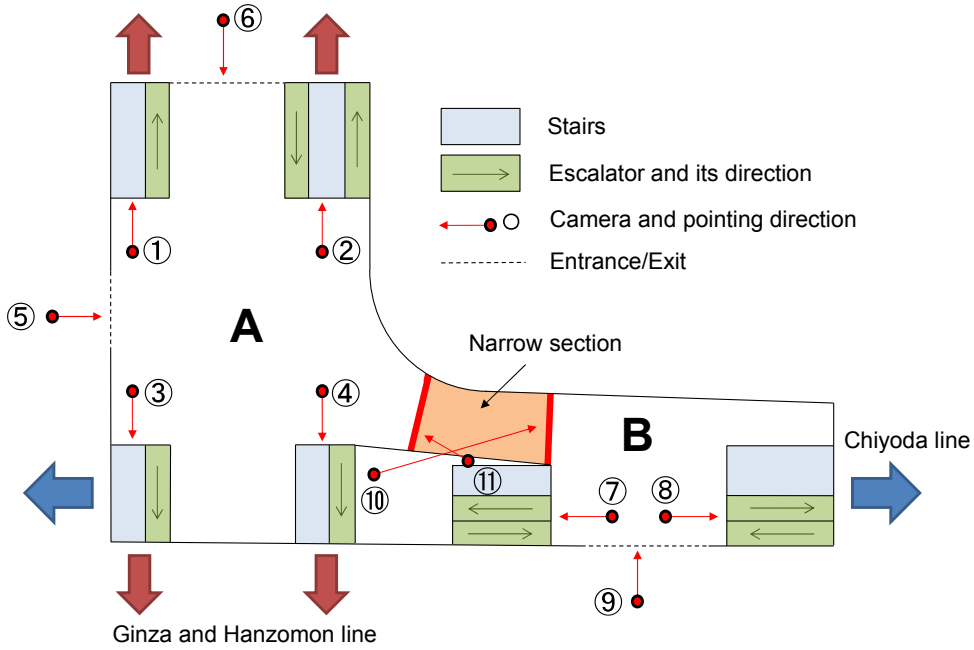

Figure 1. (color online) Schematic view of the Omote-sando subway station with number and location of each camera placed inside it and its pointing direction. The narrow section is given in red.

to work, most of them wearing black suits. Consequently, because of the low contrast between individuals, an image processing method could have led to uncertain results. Therefore, because of the above reasons, videos were analyzed manually using the open-source video processing software Kinovea.

Given the large number of people involved and the amount of video data to be processed, we decided to focus on the most relevant events during the time considered (for a single operator, analyzing 2 minutes of video for all the cameras required about 1 working day). To select these relevant events the train arrival data provided were particularly useful. In fact, it can be easily predicted that in the early morning, when ridership is low and arrivals between both concourses are out of phase, pedestrians can easily move inside the train station. On the other side, a simultaneous arrival of several trains on both concourses during rush hour may easily result in a congested motion inside the train station. More in general it can be easily predicted that after 8 AM the station will be more congested as the ridership on all lines is high.

For the above reasons, out of the 2 hours of video available only about 45 minutes were analyzed, with the selection being based on the train arrival time and a quick analysis of the video recordings obtained.

2.2. Data acquisition and treatment

The station selected, having a limited number of exits and a clear division between both concourses, makes it easy to guess the direction of each pedestrian based on the

images recorded from the cameras on-site. Since both lines connected to concourse A run parallel for a number of stations, passengers are unlikely to exchange line between them. Thus, the most likely options for a passenger getting off a train at this station are: (1) leaving the station from the closest exit or (2) moving from concourse A to B (or in the opposite direction). Entrance to the subway station is restricted by automated gates and thus other transit possibilities (entering on one side and leaving on the other,...) are very unlikely (and were observed as a very rare exception to the exchange/enter/exit main rule).
Considering the above facts, the making-up of the inflow for the narrow section in both directions starting from the single flows can be summarized as given in Figure 2(a). Each of the flows indicated in Figure 2(a) can be easily computed by using the images recorded by each camera.
In a similar way the outflow resulting in the narrow section can be obtained by knowing the flow corresponding to each camera in both concourses as indicated in Figure 2(b).

Consequently, for each camera, the number of people moving in each different direction was counted for a 5 s interval. The choice of a 5 s interval is related to practical reasons (passengers were counted manually) and to the fact that macroscopic changes (flow fluctuations,...) were found having a period longer than 15 s (thus any sampling interval smaller than this would be appropriate). A yellow tactile paving thick line (placed at the ground to allow people with impaired vision recognizing the end of stairs/escalators), was used to clearly count the passengers leaving and entering each platform. For each interval, the raw data matrix contained the number of pedestrians transiting through the camera view, categorized into their direction and the mode used (stairs/escalator) to enter/leave the platform. A sample of the data matrix for some of the cameras is given in Table 1 and Table 2.

Table 1. Data matrix containing the number of passengers passing through camera 1,3 and 9 during the given time period, categorized by their direction and moving mode (ST = stairs, ESC = escalator).

Camera		1			3			9	
Direction		To Concourse B		From Concourse B				In Station	Out Station
Mode		ST	ST	ESC	ST	ST	ESC	-	
07:59:00	07:59:05	0	0	0	0	0	0	0	0
07:59:05	07:59:10	0	0	0	1	0	2	3	1
07:59:10	07:59:15	0	0	0	1	0	0	0	0
07:59:15	07:59:20	2	0	0	0	0	0	0	0
07:59:20	07:59:25	2	0	0	3	0	0	0	2
07:59:25	07:59:30	3	0	0	4	0	4	1	1
07:59:30	07:59:35	3	0	0	9	0	2	0	2
07:59:35	07:59:40	5	0	0	8	0	3	1	1
07:59:40	07:59:45	4	0	0	4	0	1	0	0

In this way more 30'000 people transiting through the subway station during the

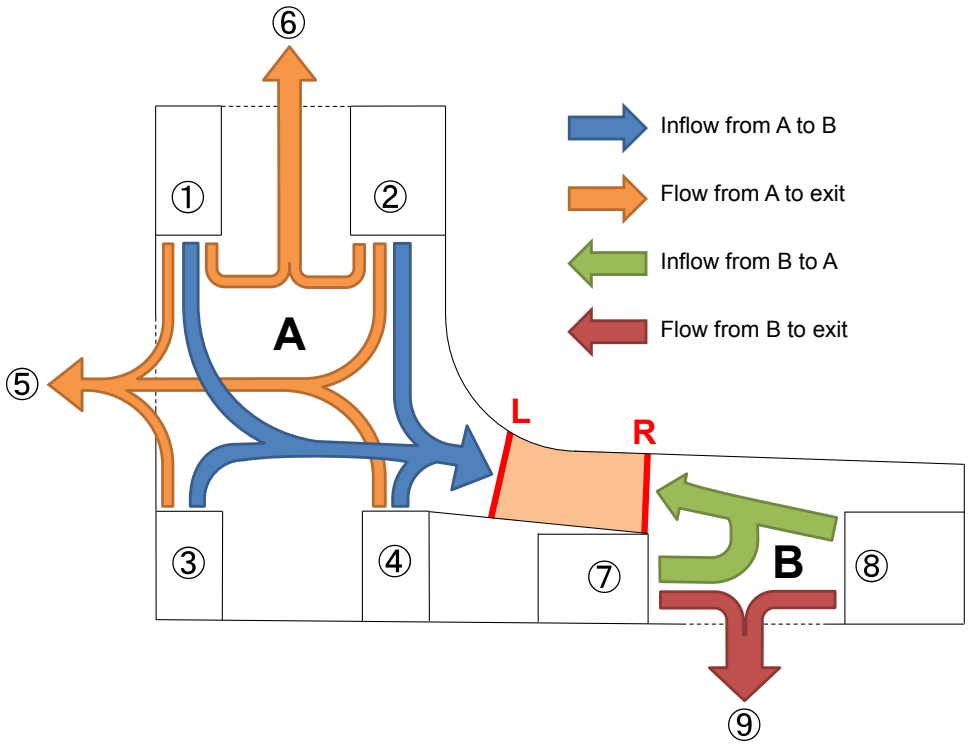

(a) Inflow composition.

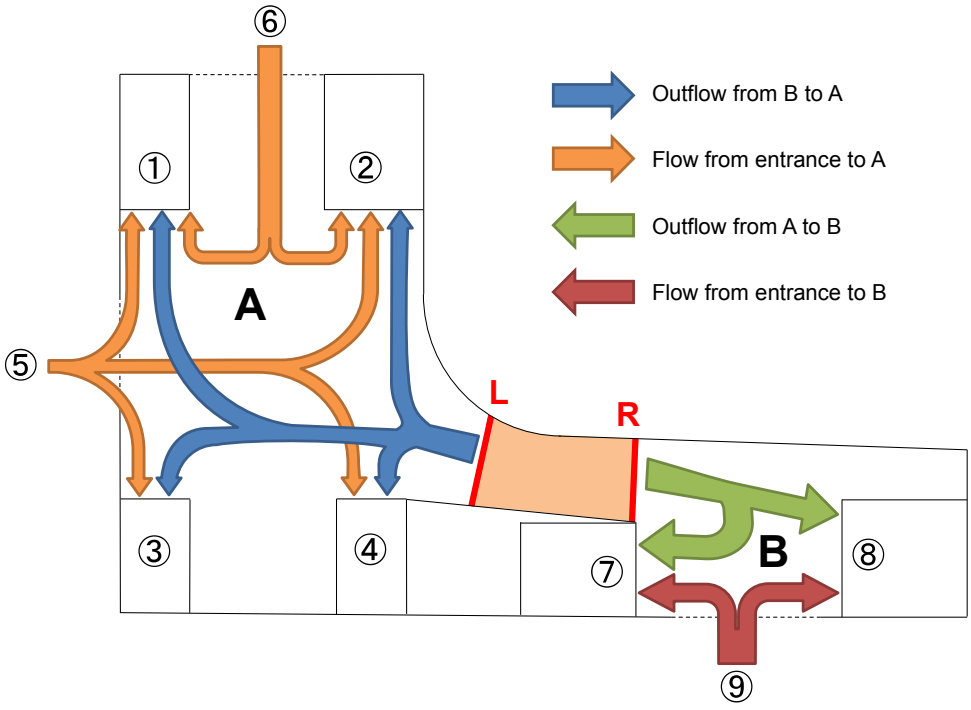

(b) Outflow composition.

Figure 2. (color online) Schematic representation of the composition of the flows resulting in the narrow section in the subway station. Numbers in circles represent the position of the corresponding cameras. L and R represent the left and right side of the narrow section.

Table 2. Data matrix containing the number of passengers passing through camera 7 and 8 during the given time period, categorized by their direction and moving mode (ST = stairs, ESC = escalator).

Camera		7				8			
Direction		To Concourse B		From Concourse B		To Concourse A		From Concourse A	
Mode		ST	ESC	ST	ESC	ST	ESC	ST	ESC
07:59:00	07:59:05	0	0	0	1	0	0	0	1
07:59:05	07:59:10	0	0	0	0	0	0	0	0
07:59:10	07:59:15	1	0	0	0	1	1	0	0
07:59:15	07:59:20	4	1	0	0	5	2	0	0
07:59:20	07:59:25	7	1	0	1	5	1	0	0
07:59:25	07:59:30	6	5	0	0	8	1	0	0
07:59:30	07:59:35	11	7	0	1	10	7	0	1
07:59:35	07:59:40	12	9	0	2	9	7	0	1
07:59:40	07:59:45	12	9	0	3	14	6	0	2

roughly 45 minutes of analysis have been counted.

Constructional setup and safety reasons constrained the position of cameras 10 and 11 (directly observing the crowded narrow section) to unfavorable locations. For these reasons people coming inside this area had to be observed from a very low height (slightly more than 2 m) and a distance of several meters. This perspective, together with the very high flow observed in this location, did not allow using the videos obtained by those cameras even in the case of manual (human operated) analysis.

As given in Figure 2(a) the inflow resulting in the narrow section can be obtained by summing up all the flows registered by the different cameras placed at the exit of each platform minus the flow of people leaving from the corresponding exits. Therefore, the total pedestrians' inflow for the narrow section in both directions can be written as:

$$\alpha_{A\to B} = \alpha_1 + \alpha_2 + \alpha_3 + \alpha_4 - \alpha_5 - \alpha_6 \tag{1}$$

$$\alpha_{B\to A} = \alpha_7 + \alpha_8 - \alpha_9 \tag{2}$$

where $\alpha_{A\to B}$ is the inflow for passengers moving from concourse A to B, $\alpha_{B\to A}$ is the same flow in the opposite direction and α_n is the flow recorded at the different locations n ($n = 1, ..., 9$).

With Figure 2(b) as reference, the outflow resulting from the flows in both directions, from concourse A to B and the opposite, can be written as:

$$\beta_{A\to B} = \beta_1 + \beta_2 + \beta_3 + \beta_4 - \beta_5 - \beta_6 \tag{3}$$

$$\beta_{B\to A} = \beta_7 + \beta_8 - \beta_9 \tag{4}$$

with β representing the outflow and the subscripts being the same for the inflow equations.

In a second step, because the distances between the narrow section and each camera

(platform connection) are different, a further adjustment had to be made to obtain the correct inflow and outflow. When computing the total inflow and outflow, the difference of time required to walk to the different destinations need to be considered.
For this purpose, for each route (for example from the left side of the narrow section L to position 4), the time required to cover the distance was obtained by checking at which time a reference person was passing through the cameras located at the corresponding locations. For each of the routes considered, 12 or more people walking at natural velocity (thus not clearly rushing) were chosen and the mean time and the standard deviation were computed as given in Table 3. For the routes leading to the exit an average value valid for the whole concourse had to be used, since in some cases passengers would use different exits (such as for position 1 or 4, where exit 5 and 6 are almost at the same distance), finally resulting in a slightly higher deviation.
The resulting walking time values were used to perform the phase shift to adjust the different flows during the total in- and outflow calculations.

Table 3. Walking time and average distance/speed for the routes considered. Note that in the case of the entrances/exits it was not possible to determine the one used by each single passenger and therefore an averaged value for the time required to leave the concourse was used. STD refers to the standard deviation.

Route	Walking time		Average		Sample size
	Average	STD	Distance	Speed	
1 ↔ L	27.3 s	3.9 s	37.9 m	1.39 m/s	12
2 ↔ L	15.3 s	2.3 s	22.2 m	1.46 m/s	12
3 ↔ L	24.9 s	3.5 s	30.7 m	1.23 m/s	12
4 ↔ L	8.7 s	2.2 s	12.4 m	1.43 m/s	12
5 ↔ L	15.4 s	2.6 s	20.2 m	1.32 m/s	24
6 ↔ L	23.0 s	4.2 s	31.4 m	1.36 m/s	24
7 ↔ B	6.4 s	2.5 s	-	-	12
8 ↔ A	15.9 s	4.7 s	-	-	24
9 ↔ A	21.4 s	5.8 s	-	-	24

The walking time obtained from the video analysis was consistent with some simple measurements performed on-site from the author by walking between different locations. In addition, the distance for each route was computed using an accurate map of the station provided by the operator (Tokyo Metro Co.,Ltd). The average walking speed obtained is consistent with the values typically found in the literature, reporting a walking speed in free flow conditions usually between 1.3-1.5 m/s [19, 20, 21].
The walking time between left and right side of the narrow section can be computed using the average walking speed and the length of the section (11.1 m, see Figure 3), resulting in about 8 s (because of the limitations imposed by the unfavorable location of cameras 10 and 11, a calculation from video frames was not possible).
To verify the reliability of the data obtained, the total number of people entering and exiting the narrow section between clearly distinct train arrivals was computed using

the tabulated data matrix compiled. If people were counted accurately and the flows had been correctly combined, than the number of people entering the narrow section in a given time period must be the same to the people leaving from the opposite side. In fluid-dynamic terms, mass conservation must be satisfied:

$$\int_{t_{start}}^{t_{end}} \alpha_{A\to B} dtdx = \int_{t_{start}}^{t_{end}} \beta_{A\to B} dtdx \tag{5}$$

$$\int_{t_{start}}^{t_{end}} \alpha_{B\to A} dtdx = \int_{t_{start}}^{t_{end}} \beta_{B\to A} dtdx \tag{6}$$

with α and β being the in- and outflow and t_{start} and t_{end} the start and end time. A discrepancy of about 2.5% was found for the number of people moving from concourse A to B and about 2.0% for the opposite direction. Considering the large number of people counted (more than 30'000) and the intermediate steps required to obtain the total in- and outflow, the accuracy reached can be considered more than satisfactory.
Finally, the phase-shifted total in- and outflow results were converted from the 5 s interval format used for simple pedestrian counting to the standard persons / m · s (from now on simply $(\mathrm{m{\cdot}s})^{-1}$) unit generally used to indicate flow in pedestrian dynamics. In doing this, the dimensions of the narrow section given in Figure 3 were used for the calculation.

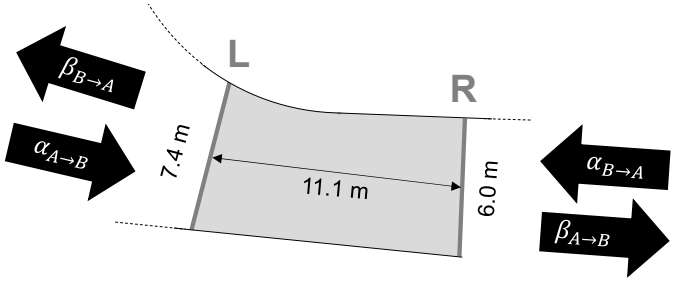

Figure 3. Dimensions of the narrow section considered. Surface is about 72 m^2.

In order to obtain clear graphs, the resulting flow was finally filtered using a low pass filter reducing the noise present in the original 5 s resolution data. Choice of the cut frequencies for the low pass filter was based on the simple criteria that noise needs to be reduced to a satisfactory level to make the results easier to read, but, on the other side, important characteristic features present in the signal needs to be preserved to allow an understanding of the phenomena observed.
In addition to the unsteady flow, we computed the cumulative curve of the number of passengers for inflow and outflow in the narrow section. By using the cumulative curve, additional information such as density and average transit time can be obtained. In particular, the vertical difference between cumulative in- and outflow gives the number of people in the narrow section at a given time (thus allowing density calculation). On the other hand, the horizontal difference between cumulative in- and outflow represents the average crossing time when the given cumulative number of people is reached.

Additionally, as we will discuss in the next section, we found the inflow ratio being an important parameter for understanding the formation of deadlocks. The inflow ratio (from now on simply flow ratio) used here is defined as:

$$r = \frac{\alpha_{A\to B}}{\alpha_{A\to B} + \alpha_{B\to A}} \tag{7}$$

where $\alpha_{A\to B}$ and $\alpha_{B\to A}$ are the inflows on both directions.

3. Results and discussion

For the most significant moments of the roughly 2 hours considered (and the 45 minutes analyzed) we computed the in- and outflow on both sides of the narrow section, the density and the flow ratio defined in Equation 7. In this section the most significant results are presented and discussed.

3.1. Free flow

In Figure 4(a) the in- and outflow for the two directions considered (from concourse A to B and the opposite direction) are represented for a free flow situation. The vertical lines visible in the figure indicate a train arrival at the given time on the corresponding concourse. As one would expect, after each arrival, there is an increase in the inflow of pedestrians in the narrow section. This is particularly clear in the case of concourse B to A, because the number of arrivals on concourse B is limited and distributed at a fairly constant rate. In the opposite direction train arrivals are more numerous and it becomes more difficult to distinguish each peak. The in- and outflow peak centers are separated by a 10 s difference, which is approximately the walking time through the narrow section (remember that the original sampling rate was 5 s).
In general it can be stated that the shape of the inflow curve, registered when passengers enter the narrow section, is quite similar to the shape of the outflow registered when they exit from the opposite side. Both can be described in term of Gaussian distribution. However, looking in detail when comparing the in- and outflow, a reduction in the flow peak height (or amplitude) and a slight increase in the width are observed in both directions. To explain this behavior one need to remember that we combined fluxes in several locations by using the average walking speed (or time, strictly speaking) to adjust the phase shift between the different signals. However, in reality, a Gaussian distribution is observed for the velocity of pedestrians [22]. In fact, observing the videos, people leaving at first the trains tend to rush toward the destination (running through the narrow section), while people leaving last tend to walk at very low pace. For this reason, even during free flow, a slight change in the flow is observed after entering the narrow section. This is particularly true in the case of movement from concourse B to A, because people leaving the test area on the left side are observed only after 20-30 s in the different cameras.
As a last consideration, it is possible to observe that there is a certain delay between the

arrivals on both concourses (simultaneous arrival are limited and the number of passengers small), thus resulting in a smooth flow during the whole time period considered.
Concerning the total flow given in Figure 4(b), similar considerations to the above remarks can be made. In particular, about 4 distinct inflow peaks are recognizable, each clearly visible in the total outflow. One can notice that the reduction in the 3rd peak is slightly more accentuated compared to the others. This may suggest some kind of slowing down, which could be linked with a weak congestion. We will talk about this below.

3.2. Congested flow

Now we will consider a different time period, for which the single and total flows are given in Figure 5.
Arrivals on both concourses are no longer delayed (as observed in the previous case). For both directions it becomes more difficult to relate each outflow peak with the inflow curve which generated it. In particular, by looking at the total flow graph, it seems that there is no relationship between both curves, except the fact that they initially grow starting from a similar time.
During this time period we observed the formation of lanes in the narrow section. In general, compared to the previous case we observed a more constrained and congested flow. People had to consider more carefully their own way, as people coming from the opposite direction were making a sort of resistance to their forward motion. However, we did not observe any deadlock here, as people did not have to significantly slow down to cross the narrow section.
It is interesting to notice, that, although slightly higher, for most of the cases the total flow in this period is comparable with the one registered in the free flow case. This suggests that the total flow alone cannot be taken as a single parameter in determining the flow regime which one will observe. For similar total flows, the flow ratio seems to play an additional role too.

3.3. Deadlock event

Finally we will analyze the cases during which deadlocks were observed. The total flow and the flow in both directions are reported in Figure 6, 7 and 8.
In the first case (Figure 6(a)), a double train arrival on both tracks connected to concourse B (arrival lines overlaps in Figure 6(a) and only a single line is visible) results in a large crowd moving to concourse A to exchange train line. The flow in that direction reaches about 1.5 $(\mathrm{m{\cdot}s})^{-1}$, more than the total flow measured during free flow. At the same time, an arrival in concourse A creates a flow of passengers moving to concourse B. The resulting inflow, although smaller than the main flow, is still remarkable, reaching a maximum of about 0.6 $(\mathrm{m{\cdot}s})^{-1}$. As a result we saw a large number of people moving simultaneously to the narrow section considered. A deadlock was clearly formed, with

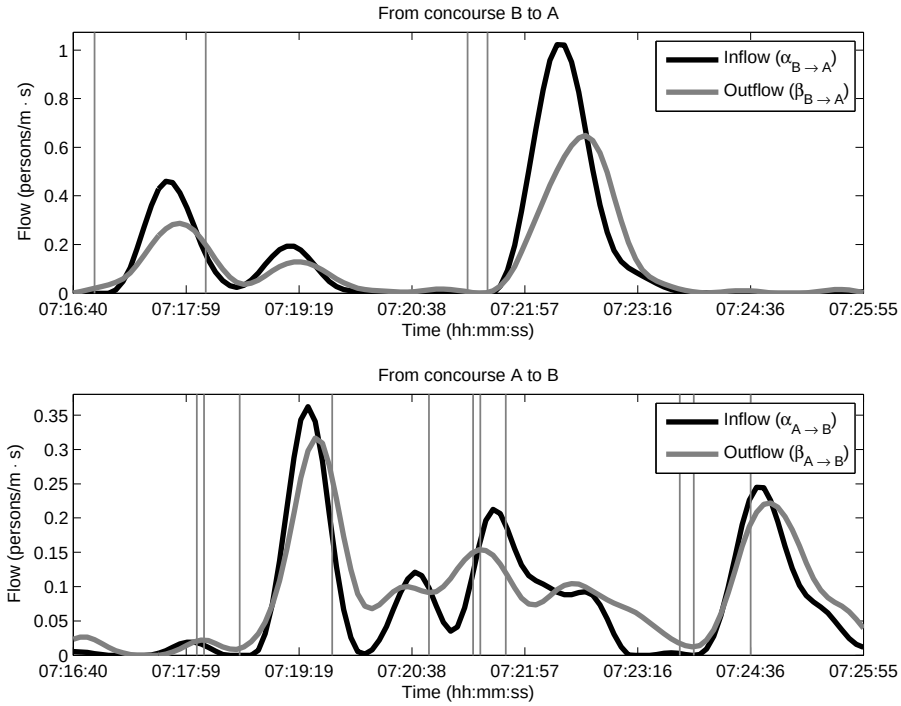

(a) In- and outflow in the different directions.

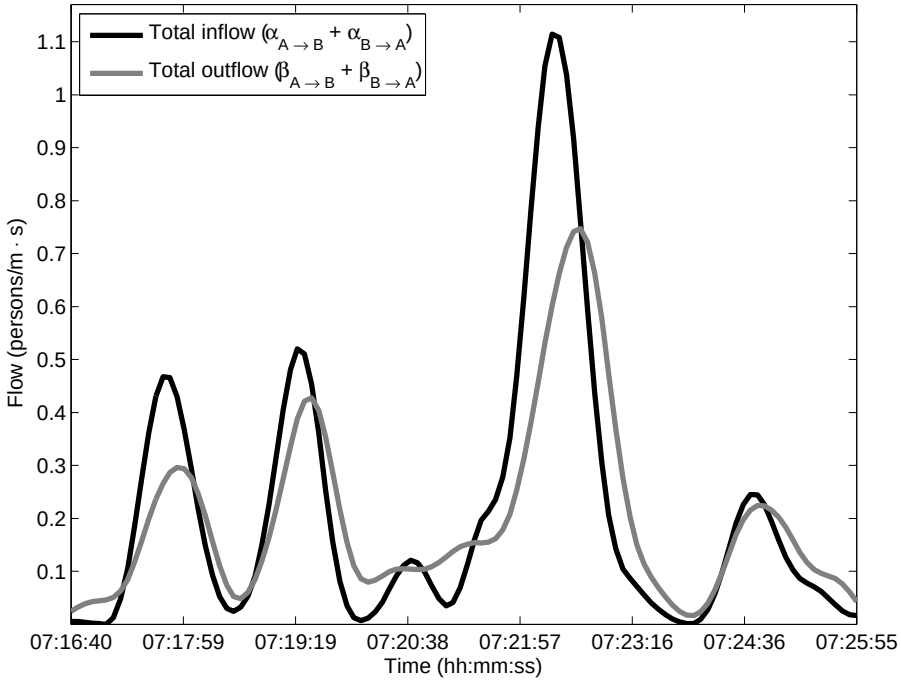

(b) Total in- and outflow in the narrow section.

Figure 4. Flow in the narrow section when free flow was observed from cameras 10 and 11.

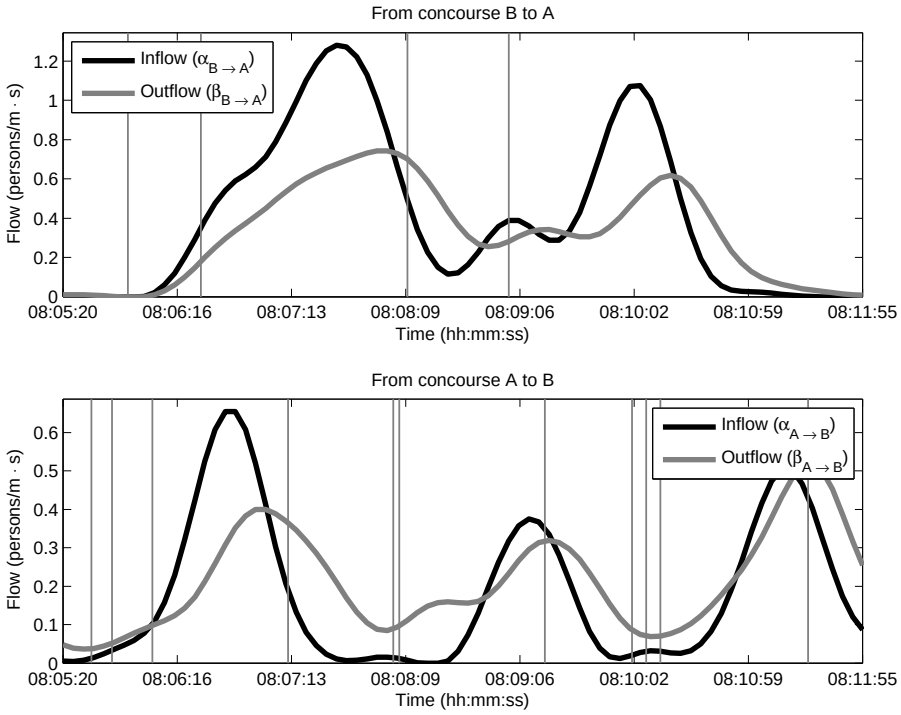

(a) In- and outflow in the different directions.

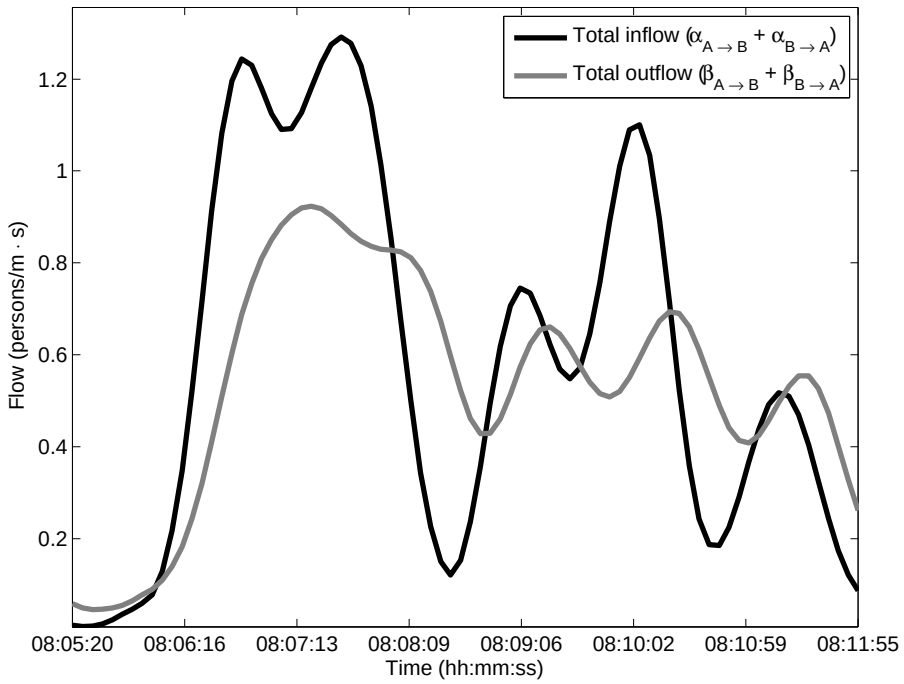

(b) Total in- and outflow in the narrow section.

Figure 5. Flow in the narrow section when congestion and lane formation was observed from cameras 10 and 11.

people in the direction A → B having to significantly slow down and briefly stop because they could not find a way through the larger crowd coming from the opposite side. By looking at both graphs in Figure 6(a) it can be noticed that inflow curves clearly grow up and decrease forming a Gaussian shape. However, a different shape is observed in the outflow: the flow first grows, then reaches a local maximum and later slightly decreases. In this portion of time some people had to stop or significantly reduce their speed, especially in the direction A → B. Later, pedestrians can find a way through the crowd, which, by becoming less dense can be penetrated easier (in a sort of percolation-like behavior). This leads to a small increase of the flow in both directions, before finally decreasing as only few passengers still have to cross the narrow section.
The same behavior was observed during another deadlock formation given in Figure 7. In this case the double peak observed in the total flow during the deadlock is even more evident. In particular, in the lower graph of Figure 7(a), it is clear that the sudden increase in the outflow (after reaching a stable value) must be related to some phenomena which happened inside the crowd, as the inflow clearly decreases in the corresponding time period.
In both cases the maximum total flow registered was close to 2.0 $(\mathrm{m{\cdot}s})^{-1}$, clearly higher than the flow we observed in free flow and congested scenarios.
A similar double peak shape was observed in different occasions during the 45 minutes analyzed (like in the time period reported in Figure 8 where two characteristic deadlock double peaks are recognized). In all the cases the deadlock formation could be recognized by looking at the cameras capturing the crowd motion in the narrow section. The largest total flow recorded in our study for the time periods considered corresponded to 2.13 $(\mathrm{m{\cdot}s})^{-1}$ (see Figure 8(b)).

3.4. Deadlock analysis

Coming back to Figure 6, it is interesting to notice that the second large peak in the direction B → A (at around 08:03) is not related to any deadlock phenomena, although its magnitude is not much different from the first peak. By carefully looking at the corresponding time period in both graphs in Figure 6(a), it can be noticed that crowd motion in both directions is smoothly shifted, thus preventing the formation of a large counter-flow. To better understand this aspect we can compare the flow ratio with the density inside the narrow section at the different times.
Figure 9(a) shows the cumulative number of people entering and leaving the narrow section during the time period corresponding to Figure 6. At the beginning the corridor was empty, thus creating the necessary conditions for the analysis based on the cumulative graphs.
First, both the cumulative inflow and outflow grow as people enter the narrow section and promptly leave from the opposite side. After a short time cumulative inflow grows more rapidly, therefore indicating that someone needs more time to cross the section and people start to accumulate within it. After a while both curves become closer again

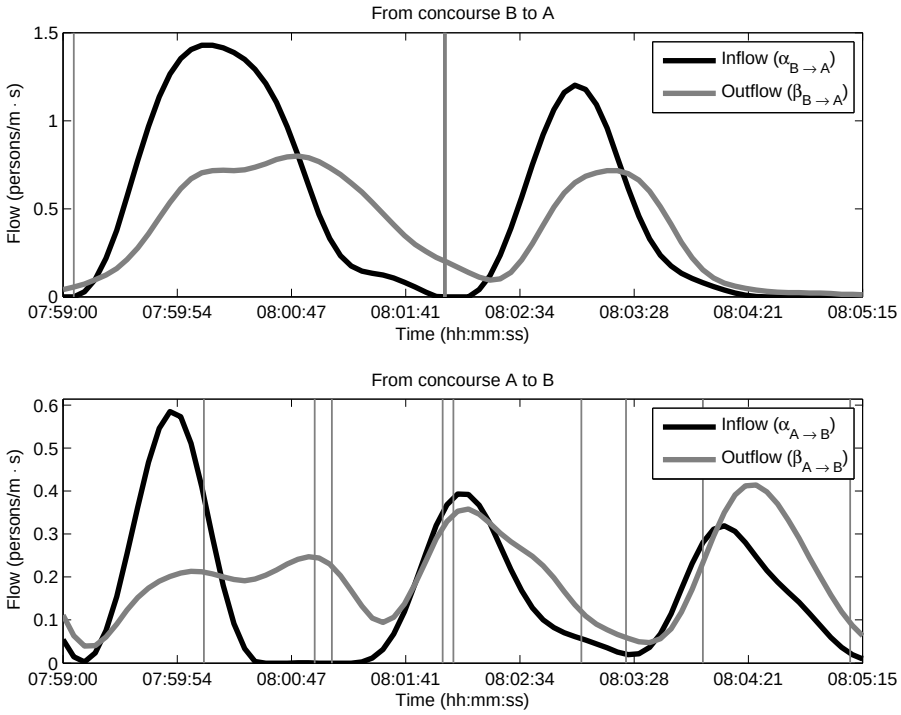

(a) In- and outflow in the different directions.

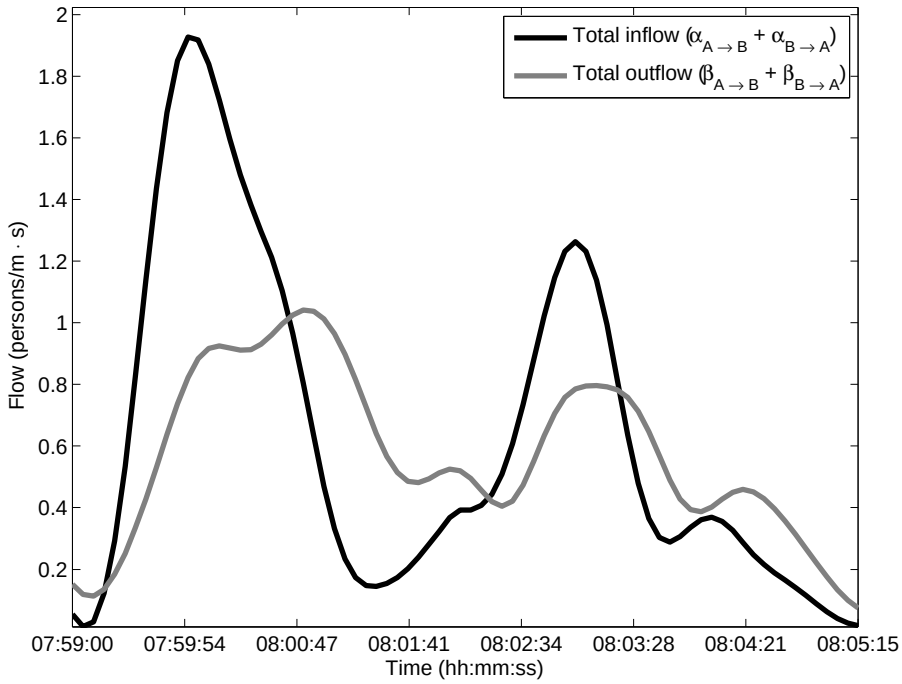

(b) Total in- and outflow in the narrow section.

Figure 6. Flow in the narrow section when deadlock was observed from cameras 10 and 11.

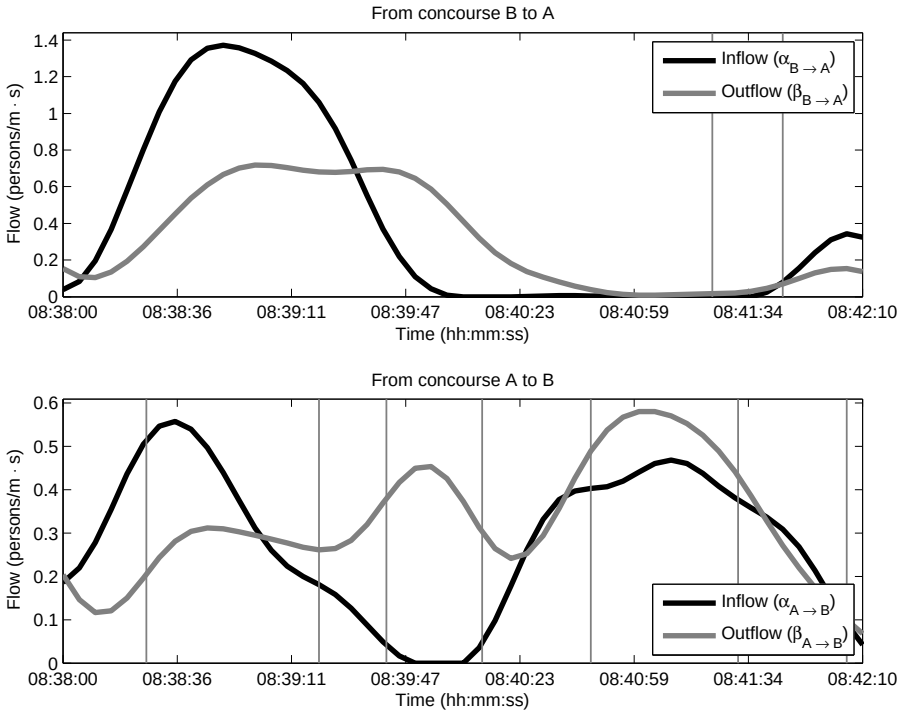

(a) In- and outflow in the different directions.

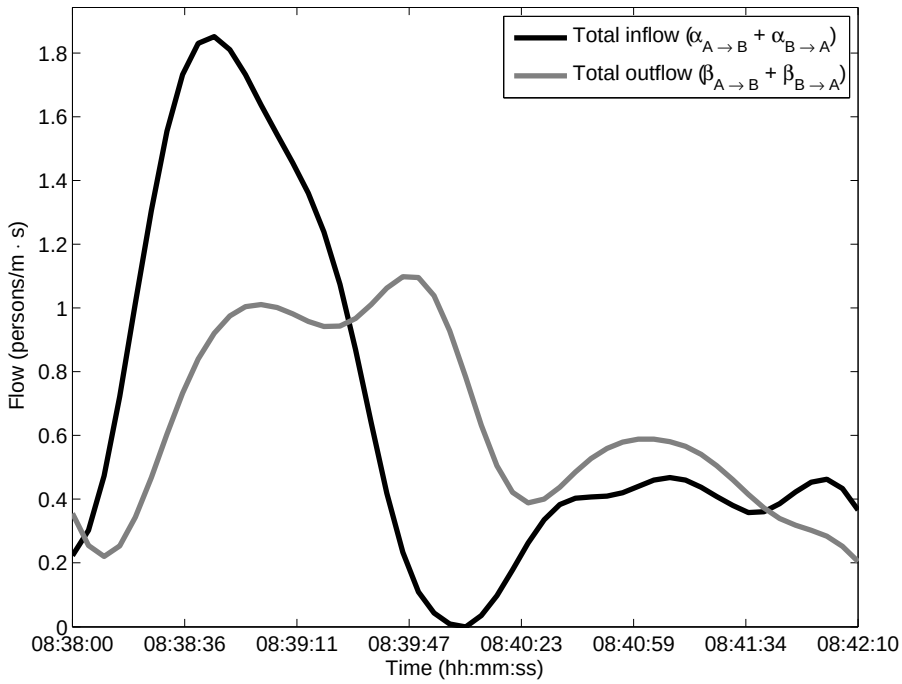

(b) Total in- and outflow in the narrow section.

Figure 7. Flow in the narrow section when deadlock was observed from cameras 10 and 11.

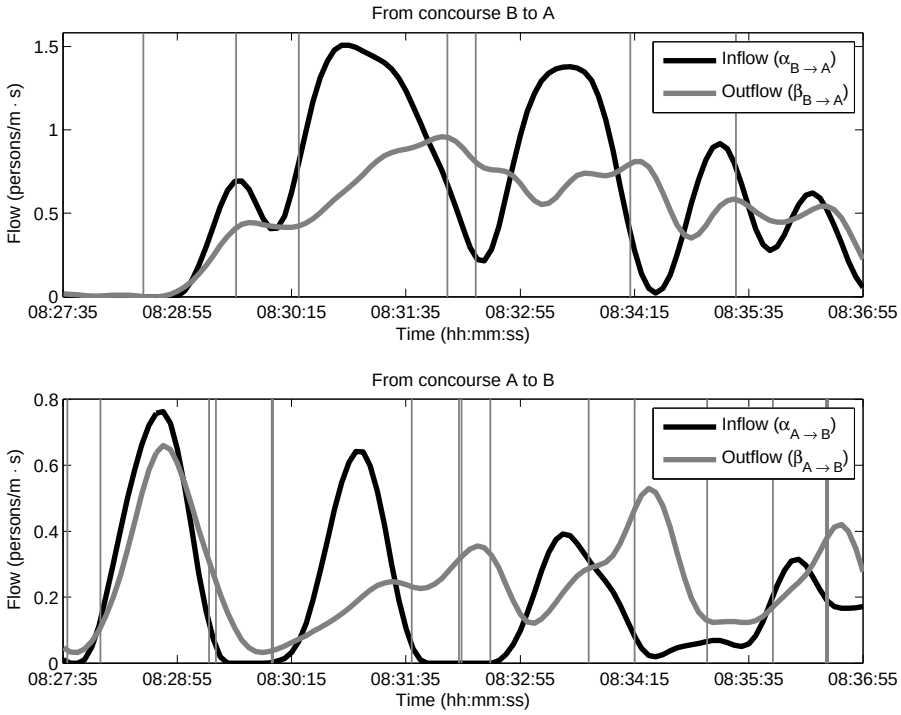

(a) In- and outflow in the different directions.

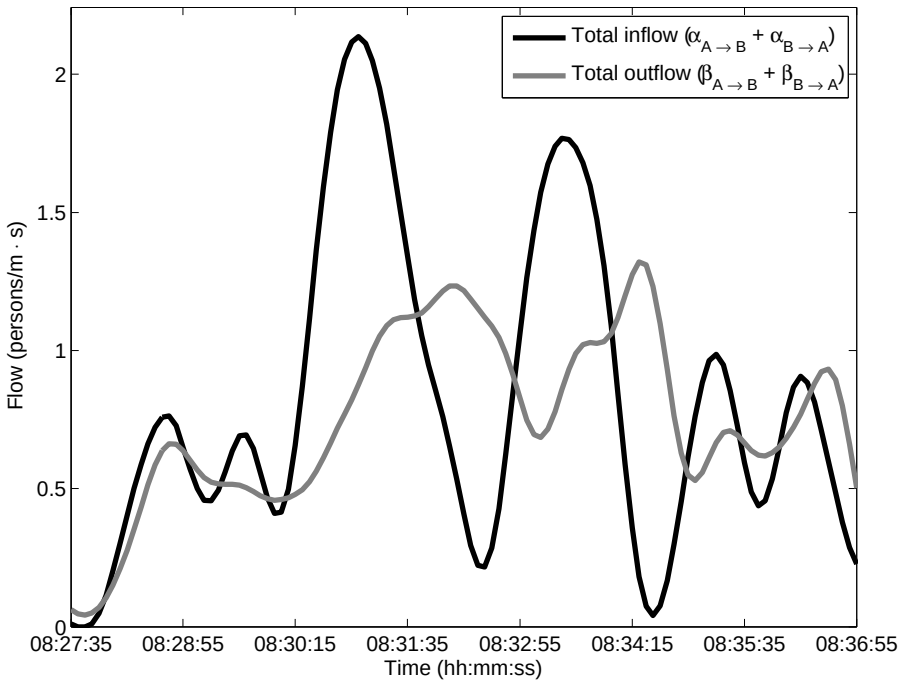

(b) Total in- and outflow in the narrow section.

Figure 8. Flow in the narrow section when the maximum inflow was recorded (deadlocks were observed).

as the flows in both direction approaches zero. Later, a new set of train arrivals lead to a new increase of both curves to finally converge again when the corridor empties. The small difference visible at the end of the curves is related to the previously discussed error resulting from manually counting the passengers and combining the data of the different cameras (about 2% here).
The vertical difference of both curves in Figure 9(a) gives the number of people in the narrow section at any given time, which divided by its surface, gives the density indicated in gray in Figure 9(b). By comparing this curve with the flow ratio, it can be observed that a steep increase in the density is found when the flow ratio is close to 0.5 (balanced flow in both directions). In fact, in the first half of the graph, when the flow ratio reaches a value of about 0.3 a steep density increase occurs. In the second peak the flows in both directions are less balanced, thus preventing a sudden increase of the density inside the narrow section. A similar behavior was observed in different time periods corresponding to highly crowded situations.
The same type of phenomenon is observed for the time period corresponding to Figure 8, for which the cumulative curve, the density and the flow ratio are reported in Figure 10. Like in the previous case, even here, the increase in density after 08:30:15 is associated with an increase of the flow ratio, meaning that a counter flow is obstructing the motion of the pedestrians in the main flow. Although the flow is not perfectly balanced, it seems that under extreme conditions (high unidirectional flow) a small amount of counter flow can quickly lead to a density increase, as pedestrians find it more difficult to pass the incoming crowd. A similar event is observed after 08:32:55 when another deadlock occurred.
Concluding, as previously suggested, we confirmed that the formation of deadlocks is obviously related with the total flow, but flow ratio plays an important role and therefore needs to be considered closely.

3.5. Flow regime categorization

Besides the importance of the flow ratio in pedestrian bidirectional flow, we found that there is a connection between the in- and outflow curves and the type of flow observed. In the case a finite crowd crosses a corridor in opposite directions, the type of flow observed can be described by looking at the shape of the recorded outflow, as schematically given in Figure 11. In the case of free flow a Gaussian inflow curve will result in a very similar curve in the outflow. In a congested scenario (with lane formation), the shape of the outflow curve will change, but a single peak Gaussian curve will still be recognizable. When deadlock occurs a curve including a double peak is observed instead.

Because tracking information such as position or speed were not available for each pedestrian, we could not use numerical indexes such as the order parameter [23] to classify each flow regime. Therefore we decided to classify the flow regime for each inflow-outflow combination (which is roughly corresponding to single or very close train arrivals) based on the qualitative information contained in the video. Concerning the

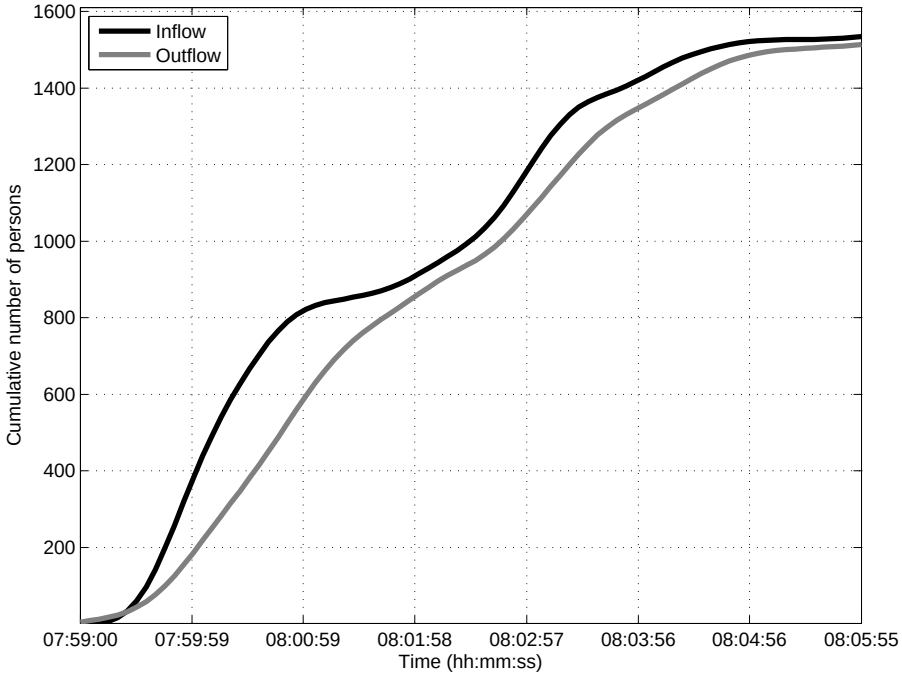

(a) Cumulative in- and outflow in the narrow section.

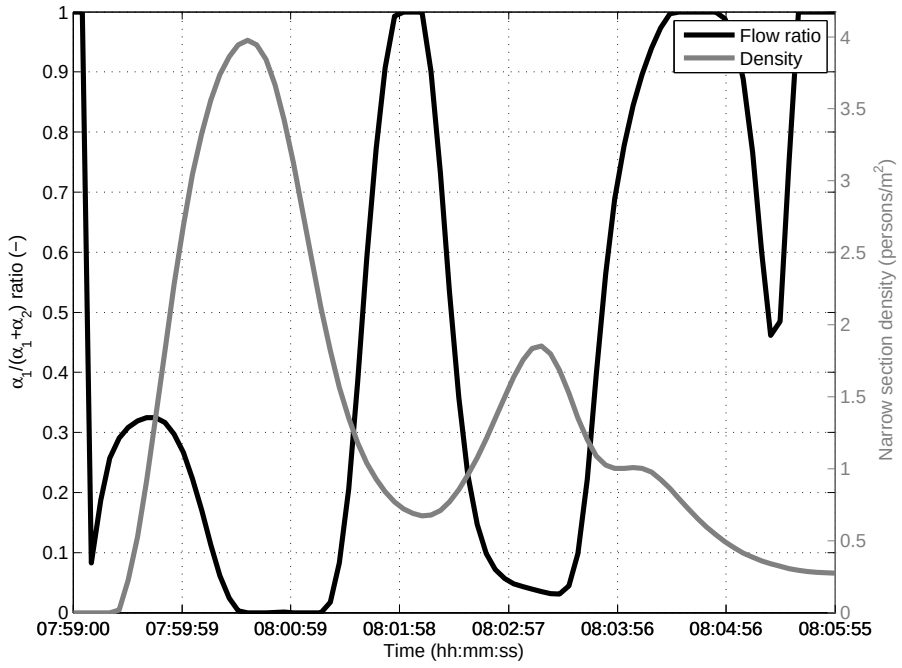

(b) Flow ratio and density in the narrow section.

Figure 9. Cumulative flow, flow ratio and density during a deadlock event.

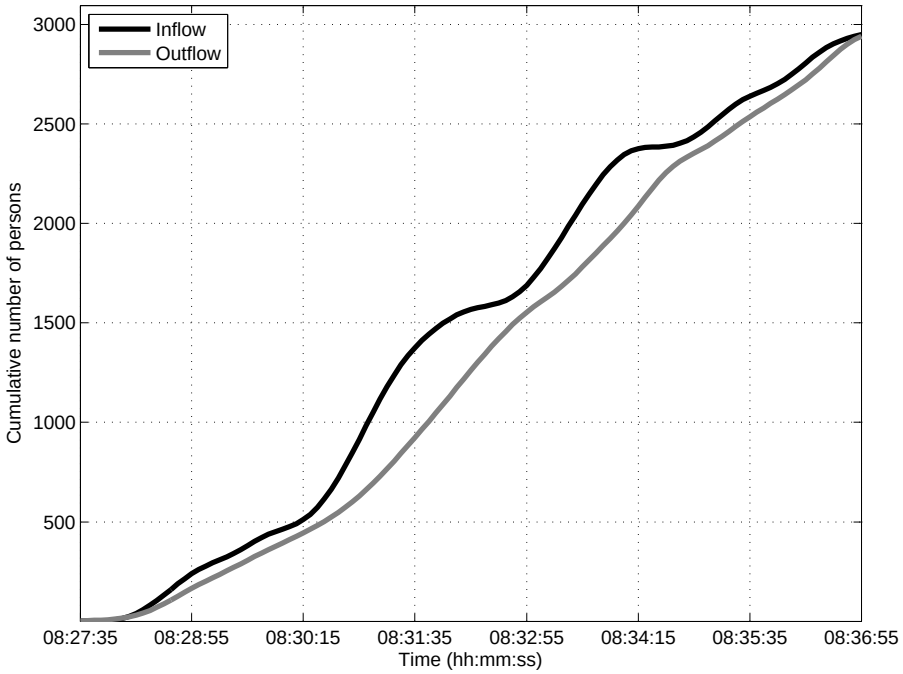

(a) Cumulative in- and outflow in the narrow section.

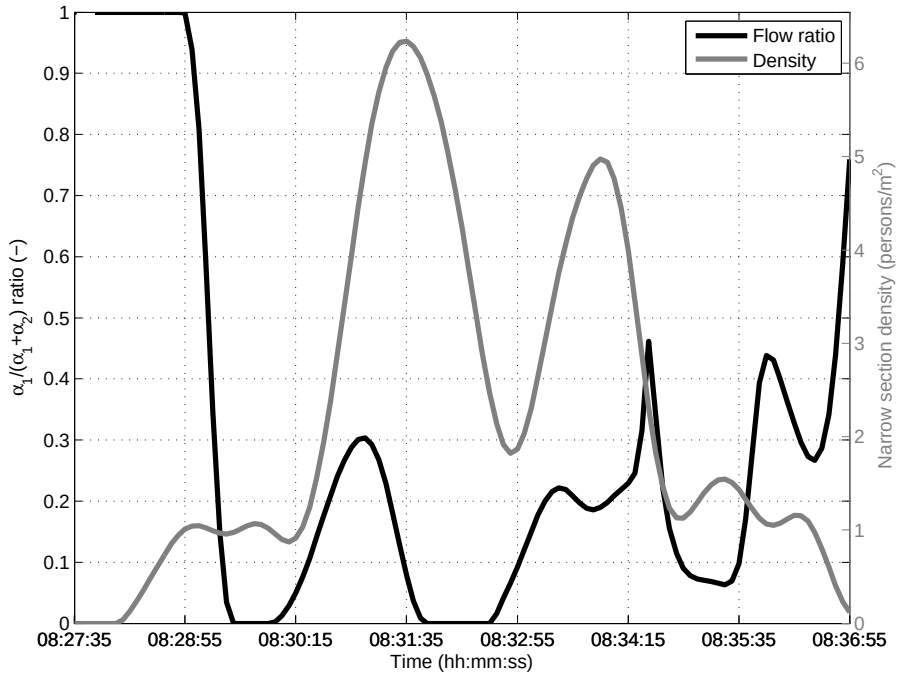

(b) Flow ratio and density in the narrow section.

Figure 10. Cumulative flow, flow ratio and density during a deadlock event.

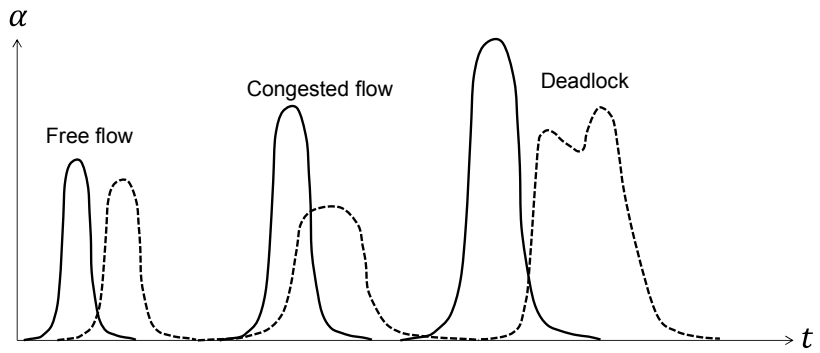

Figure 11. Type of flow categorized based on the shape of the in- and outflow.

inspection of the videos, categorization was carried out based on the following qualitative criteria:

- Free flow: pedestrians move in complete freedom and there is not any correlation between the movement of the individuals. Distinctive feature of this flow regime is that pedestrians can turn easily because their motion is not constrained by the surrounding crowd.
- Congested flow: some collective behavior is observed in the crowd, the most prominent being the spontaneous formation of lanes. Walking speed in this case is not significantly different from free flow, but lateral movements are constrained.
- Deadlock: several pedestrians have to stop or significantly slow down because of the large crowd created and the strong counter-flow. The slowing down/stopping behavior is usually observed in the minor flow.

In general we found a good agreement between the criteria based on flow curves and the qualitative recognition. In particular, all the characteristic double peaks were found being related to deadlocks, with pedestrians having to stop or significantly slow down. Distinction between free flow and congested flow was more difficult, especially considering that analysis was originally based on qualitative criteria. However, we found that it is possible to set a quantitative criterion to distinguish between free flow and congested flow. In fact, when the difference between the in- and outflow peak was less than 0.25 $(\mathrm{m{\cdot}s})^{-1}$, free flow was observed. A peak difference larger than 0.25 $(\mathrm{m{\cdot}s})^{-1}$ with a single peak corresponded to congested flow. The 0.25 $(\mathrm{m{\cdot}s})^{-1}$ flow drop (difference) criterion is successfully discriminating the categorization based on qualitative aspects.

Figure 12 shows the categorization of the flow regime plotted against the single flows in both directions ($\alpha_{A\to B}$ and $\alpha_{B\to A}$). Although the limited number of observations, a distinction could be made between the different flow regimes. In particular, considering the several points available for free flow and congested flow a clear partition could be drawn. In this regard a semicircle was found discriminating with better accuracy both data sets compared to a linear division. Concerning congested flow and deadlock we did

not have enough points to draw a distinguishing partition between both flow regimes. However, it is known from the literature that the limit for unidirectional flow is about 2.2 $(\mathrm{m{\cdot}s})^{-1}$ [24, 25, 11]. By looking at the data shown in Figure 12, it is clear that a straight line passing through those two points cannot distinguish between the different flow regimes. In contrast, a semicircle allows using the unidirectional flow limits and the experimental data to discriminate congested flow and deadlock formation with sufficient accuracy.

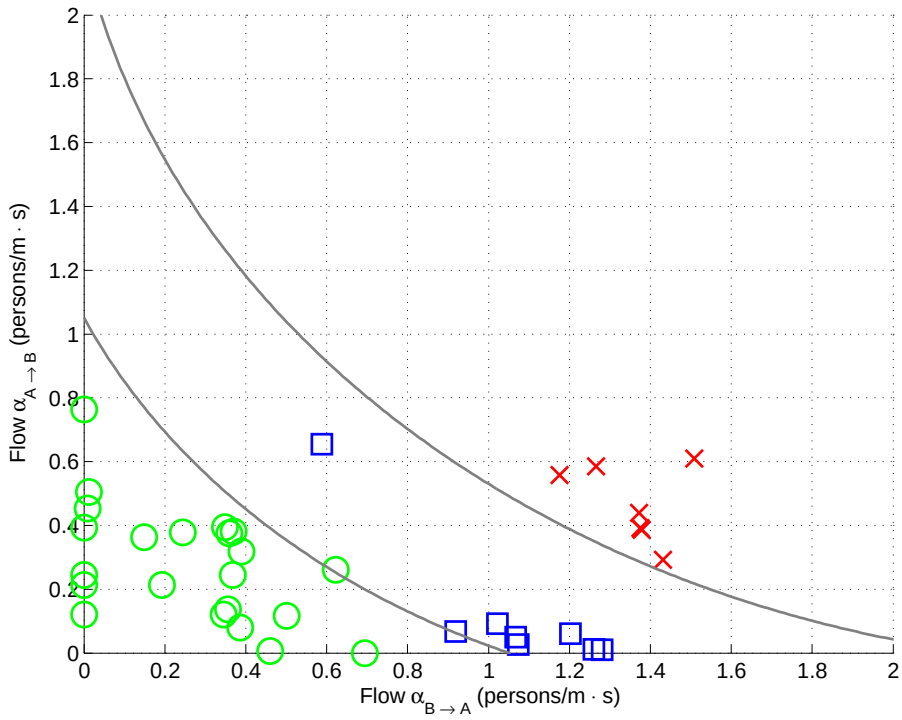

Figure 12. (color online) Flow regime categorization in the case of pedestrian bidirectional flow (circle = free flow, square = congested flow, cross = deadlock).

As reported above, semicircles were found fitting well the boundaries between the different flow regime regions. The equation for the boundaries can be written as:

$$(\alpha_{A\to B} - c_{AB})^2 + (\alpha_{B\to A} - c_{BA})^2 = r^2 \tag{8}$$

with c_{AB} and c_{BA} being the coordinate of the center of the semicircle and r its radius. For both boundaries considered the equation's parameters, the maximum (unidirectional) flow and the minimum (bidirectional) flow are given in Table 4.

Clearly flow ratio plays an important role in determining the flow regime, as partition between the different regions is not linear. In fact, transition between one flow regime and the next one occurs earlier (i.e. at lower total flow) in the regions corresponding to a balanced flow. For the discrimination between the regions of different point sets, we found curved lines fitting better than straight lines, thus highlighting the role of flow ratio in the understanding of pedestrian bidirectional flow.

Table 4. Parameters for the flow regime boundaries: α_{max} is the maximum (unidirectional) flow and α_{min} is the minimum (bidirectional) flow. Units are $(\mathrm{m{\cdot}s})^{-1}$.

Boundary	c_{AB}	c_{BA}	r	α_{max}	α_{min}
Free flow / Congested	1.853	1.853	2.019	1.05	0.85
Congested / Deadlock	2.654	2.654	2.692	2.20	1.50

4. Comparison with previous research

Most of the literature available for pedestrian flow is focused on unidirectional motion, with a special regard to evacuation. Only a limited number of researchers have been studying bidirectional pedestrian flows in detail, with most of the studies dealing with numerical simulation. In particular, concerning cellular automata, the works by Blue et al. and Tajima et al. provided a wide perspective of bidirectional flows [26, 27] in a numerical way.

For comparison with the study presented here we will mainly focus on previous experimental works. In this regard, four different experimental works and one numerical study will be taken into consideration here. In this section one has to remind that a direct comparison with previous research is difficult because in this study total flow and flow ratio changes rapidly, providing a new inside into unsteady conditions, but making direct comparisons more challenging.

In addition, it is necessary to remark that although previous studies were able to predict flow capacity by analyzing the behavior of parameters such as crossing time and average walking speed, the existence of those limit could not be confirmed through actual observation of critical scenarios such as deadlock formation.

4.1. Crosswalks observation by Lam et al.

Lam et al. [16, 17] observed pedestrian behavior at crosswalks in different locations in Hong Kong. Based on video recordings, average crossing time and resulting total flow were measured. Lam et al. concluded that the relationship between the flow capacity and the flow ratio in the case of crosswalks can be approximated by a third order polynomial function. In particular they found that a limited amount of counter-flow deteriorates the overall performance, but under balanced conditions stable lanes will be formed thus reducing the friction between individuals and increasing the resulting capacity.

Although numerical data for density are not directly given, sample pictures provided, suggest that the observation was carried out under low densities. In addition, in contrast to a corridor, pedestrians crossing a crosswalk are able to walk outside the signalized path in case the density becomes high. For this reasons, numerical results obtained by Lam et al. are not directly comparable with the current research, but, in accordance to our results, his analysis suggests that flow capacity and flow ratio have a non-linear

relationship.

4.2. Experiments by Kretz et al.

Kretz et al. [14] performed a supervised experiment with about 65 people crossing a corridor in opposite directions. Width of the test section of the corridor was about 2 m and its length about 10 m. Three cameras were placed at the beginning, the center and the end of the test section for data collection. Kretz et al. concluded that the sum of flows in bidirectional situations is always larger than the flow observed in unidirectional cases. However, this conclusion may be related to the different ways in which unidirectional and bidirectional flows are considered. Concerning flow ratio, Kretz et al. found the balanced flow performing worst, in agreement with our observation. In addition, a non-linear relationship between total flow and flow ratio was reported. Absolute values for maximum flow were higher than the one given here and generally higher than the overall literature.

4.3. Drag force model by Alhajyaseen et al.

Alhajyaseen et al. [28, 29] developed a drag force model based on observations of crosswalks in different locations in Nagoya. They concluded that the balanced flow performs the worst and the unidirectional flow has the highest capacity. In addition, the flow capacity - flow ratio relationship they obtained is in very good agreement with the results presented here. However, the function that Alhajyaseen et al. developed converges to infinity for unidirectional flow and a transition from unidirectional to bidirectional flow cannot be described numerically.

4.4. Experiments by Zhang et al.

Zhang et al. [11, 30] performed a bidirectional flow experiment in a mock corridor with a large number of participant (about 350) and, by placing a camera on azimuthal direction above the ground, were able to track pedestrians' position, thus obtaining accurate data for flow, density and velocity. Based on those data they constructed several fundamental diagram for bidirectional flow. Although flow ratio is not strictly considered in their research, a simple comparison with the present study is possible. In particular, Zhang et al. concluded that counter-flow reduce the maximum total flow and the lowest value is about 1.5 $(\mathrm{m{\cdot}s})^{-1}$ in the case of balanced flow, well in agreement with the results reported here.

4.5. Bidirectional flow analysis by Nowak et al.

Nowak et al. [23] studied bidirectional pedestrian flow using a cellular automaton model and an order parameter (based on colloidal suspensions) to detect lane formation. In their study they identified four different states: free flow, disordered flow, lane formation and gridlock (called deadlock here). The order parameter was particularly useful to

distinguish between disordered flow (without lanes) and lane formation. In this study, because individual position and velocity for each pedestrian were not available, the two states could not be distinguished. Nonetheless, the categorization proposed by Nowak et al. is in line with the flow regime subdivision proposed here. Unfortunately, a quantitative comparison between both works is not possible, because the analysis by Nowak et al. is mostly focused on simulation parameters and qualitative aspects.

5. Conclusions

Most of the articles reported in the literature present studies which are either numerical (and therefore difficult to relate with real-life phenomena) or experimental investigations performed under precisely determined conditions. In this study we reported the results of an observation without particular constraints, with participants behaving in a completely natural way.

By analyzing the motion of pedestrians crossing a narrow section from opposite directions, we observed characteristic shapes in the curves of total in- and outflow. When a group of pedestrians crossed the test section, a typical Gaussian curve was formed in the total inflow (as a consequence of the velocity distribution being also Gaussian). The outflow curve, however, had different shapes depending on the phenomena which occurred in the test section. For instance, a Gaussian peak having height and width similar to the the one observed for the inflow indicates that free flow occurred. The widening of the width in combination with a reduction of the peak's height signals a congested flow. The observation of a double peak combination in the outflow (although this characteristic was not present in the inflow curve) points out the formation of a deadlock during the given time.

In addition, in this study, we confirmed the importance of the flow ratio for determining the flow regime at a given total flow. Based on the flow results, our research allowed to sketch a flow regime diagram for pedestrian bidirectional flow distinguishing between different flow regimes depending on flow and counter-flow. In that context, flow ratio was found having a non-linear relationship in regard with transition between one regime to the next (and to determine the flow capacity). However, the exact relationship between total flow and flow ratio still need to be determined and can be a topic for future research.

This study can be relevant for understanding the phenomenological distinction between different flow regimes and can provide important data to validate and develop numerical codes used for the prediction of these phenomena.

Acknowledgment

The authors wish to thank Tokyo Metro Co.,Ltd for allowing us to record the crowd in Omote-sando station and for assisting us with the experimental part of this study.

This work was financially supported by JSPS KAKENHI Grant Number 25287026 and

the Doctoral Student Special Incentives Program (SEUT RA) of the University of Tokyo.

References

[1] Fruin J J 2002 The causes and prevention of crowd disasters *First International Conference on Engineering for Crowd Safety* pp 1–10

[2] Helbing D and Mukerji P 2012 *EPJ Data Science* **1** 1–40 ISSN 2193-1127 (*Preprint* 1206.5856v1)

[3] Boari S, Josens R and Parisi D R 2013 *PLoS ONE* **8** 1–7 ISSN 19326203

[4] Altshuler E, Ramos O and Nu Y 2014 *The American Naturalist* **166** 643–649

[5] Garcimartín A, Pastor J M, Ferrer L M, Ramos J J and Zuriguel I 2015 *Physical review. E, Statistical, nonlinear, and soft matter physics* **022808** 1–7

[6] Saloma C, Perez G J, Tapang G, Lim M and Palmes-Saloma C 2003 *Proceedings of the National Academy of Sciences of the United States of America* **100** 11947–11952 ISSN 0027-8424

[7] Piccoli B and Tosin A 2009 *Continuum Mechanics and Thermodynamics* **21** 85–107 ISSN 09351175 (*Preprint* 0812.4390)

[8] Helbing D and Molnár P 1995 Social force model for pedestrian dynamics (*Preprint* 9805244)

[9] Kirchner A and Schadschneider A 2002 *Physica A: Statistical Mechanics and its Applications* **312** 260–276

[10] Bandini S, Federici M L, Manzoni S and Vizzari G 2006 *Lecture Notes in Computer Science (including subseries Lecture Notes in Artificial Intelligence and Lecture Notes in Bioinformatics)* **3963 LNAI** 203–220 ISSN 03029743

[11] Zhang J, Klingsch W, Schadschneider A and Seyfried A 2011 *Journal of Statistical Mechanics* **02002** 9 ISSN 1742-5468 (*Preprint* 1107.5246) URL http://arxiv.org/abs/1107.5246

[12] Suma Y, Yanagisawa D and Nishinari K 2012 *Physica A: Statistical Mechanics and its Applications* **391** 248–263 ISSN 03784371 URL http://linkinghub.elsevier.com/retrieve/pii/S0378437111005693

[13] Yanagisawa D, Nishi R, Tomoeda A, Ohtsuka K, Kimura A, Suma Y and Nishinari K 2010 *SICE Journal of Control, Measurement, and System Integration* **3** 395–401 URL http://yana.sci.ibaraki.ac.jp/CV/Papers/JCMSI_03_0395_2010.pdf

[14] Kretz T, Grünebohm A, Kaufman M, Mazur F and Schreckenberg M 2006 *Journal of Statistical Mechanics* ISSN 1742-5468 (*Preprint* 0609691) URL http://arxiv.org/abs/cond-mat/0609691

[15] Karamouzas I, Skinner B and Guy S J 2014 *Phys. Rev. Lett.* **113**(23) 238701 URL http://link.aps.org/doi/10.1103/PhysRevLett.113.238701

[16] Lam W H K, Lee J Y S and Cheung C Y 2002 *Transportation* **29** 169–192 ISSN 00494488

[17] Lam W H K, Lee J Y S, Chan K S and Goh P K 2003 *Transportation Research Part A: Policy and Practice* **37** 789–810 ISSN 09658564

[18] 2012 Tokyo metropolitan government, tokyo statistical yearbook 2012

[19] Seyfried A, Steffen B, Klingsch W and Boltes M 2005 *Journal of Statistical Mechanics* **10002** 13 ISSN 1742-5468 (*Preprint* 0506170) URL http://arxiv.org/abs/physics/0506170

[20] Chandra S and Bharti A K 2013 *Procedia - Social and Behavioral Sciences* **104** 660–667 ISSN 18770428 URL http://linkinghub.elsevier.com/retrieve/pii/S1877042813045515

[21] Finnis K K and Walton D 2008 *Ergonomics* 37–41

[22] Saberi M, Aghabayk K and Sobhani A 2015 *Physica A: Statistical Mechanics and its Applications* **434** 120–128 ISSN 03784371 URL http://linkinghub.elsevier.com/retrieve/pii/S0378437115003672

[23] Nowak S and Schadschneider A 2012 *Physical Review E* **85** 1–11 (*Preprint* arXiv:1206.3084v1)

[24] Kretz T, Gruenebohm A and Schreckenberg M 2006 *Journal of Statistical Mechanics* **2006** ISSN 1742-5468 (*Preprint* 0610077)

[25] Seyfried A, Rupprecht T, Passon O, Steffen B, Klingsch W and Boltes M

2009 *Transportation Science* **43** 16 ISSN 0041-1655 (*Preprint* 0702004) URL http://arxiv.org/abs/physics/0702004

[26] Blue V J and Adler J L 2000 *Proc. Artificial Life VII* 437–445

[27] Tajima Y, Takimoto K and Nagatani T 2002 *Physica A: Statistical Mechanics and its Applications* **313** 709–723 ISSN 03784371

[28] Alhajyaseen W and Nakamura H 2009 *Proceedings of Infrastructure Planning* **39** 3–6

[29] Alhajyaseen W K M, Nakamura H and Asano M 2011 *Procedia - Social and Behavioral Sciences* **16** 526–535 ISSN 18770428 URL http://dx.doi.org/10.1016/j.sbspro.2011.04.473

[30] Zhang J, Schadschneider A and Seyfried A 2014 Empirical Fundamental Diagrams for Bidirectional Pedestrian Streams in a Corridor *Pedestrian and Evacuation Dynamics 2012* (Springer) pp 245–250 ISBN 9781441997241 URL http://www.springerlink.com/index/10.1007/978-1-4419-9725-8